The Effect of Coating Procedure on the Strength and Corrosion Resistance of Epoxy Coatings on A36 Steel: Pull-Out and Potentiodynamic Analysis

Teguh Dwi Widodo
Mechanical Engineering Department, Universitas Brawijaya, Malang, Indonesia
widodoteguhdwi@ub.ac.id (corresponding author)

Redi Bintarto
Mechanical Engineering Department, Universitas Brawijaya, Malang, Indonesia
redibintarto@ub.ac.id

Putu Hadi Setyarini
Mechanical Engineering Department, Universitas Brawijaya, Malang, Indonesia
putu_hadi@ub.ac.id

Rudianto Raharjo
Mechanical Engineering Department, Universitas Brawijaya, Malang, Indonesia
rudiantoraharjo@ub.ac.id

Ilham Dwi Darmawan
Mechanical Engineering Department, Universitas Brawijaya, Malang, Indonesia
Ilham@ub.ac.id

Received: 19 May 2025 | Revised: 10 July 2025 | Accepted: 27 July 2025

 DOI: https://doi.org/10.48084/etasr.12259

ABSTRACT

In harsh environments with a high chloride ion content, a high-performance coating must be applied to steel. For the latter to be protected in such conditions epoxy coating is often used. The performance of this coating depends on its type and the application process. Corrosion resistance and adhesion are considered important parameters in this process. This study investigates the impact of coating application methods (spray (S), handroll (H), and combinations (S+H)) on the epoxy coating performance on ASTM A36 steel substrates. A mathematical model of void formation during the drying processes is also presented. A combined garnet blasting and high-pressure water blasting method was employed to achieve optimal substrate cleanliness and roughness prior to the coating processes. The coating quality and mechanical integrity were characterized by pull-out adhesion testing and potentiodynamic polarization analysis in chloride-rich water. The results demonstrated notable differences influenced by the coating application technique. The H+S showed the highest adhesion strength (13.05 MPa), primarily due to improved primer-substrate, mechanical interlocking, and minimized void content. On the other hand, S+H showed the lowest adhesion strength, which was explained by weaker primer-substrate bonding and increased porosity. Testing using potentiodynamic polarization revealed that the coatings applied only by (H+H) had the best corrosion resistance, as evidenced by their lowest corrosion current density and most positive corrosion potential. The (S+S), on the other hand, produced the least amount of corrosion resistance.

Keywords-epoxy coating; corrosion; pullout strength; spray; handroll

I. INTRODUCTION

The utilization of epoxy coatings in shipbuilding has attracted significant interest as a result of their exceptional features, including corrosion protection, durability, and the ability to be applied to a variety of surfaces [1-3]. The marine environment poses substantial challenges for materials, particularly in terms of corrosion caused by salinity, operating conditions, and temperature fluctuations. The significance of epoxy coatings in maritime applications is underscored by research on their adhesive strength and corrosion resistance, emphasizing their benefits in safeguarding the ship structures [4]. Epoxy coatings have been extensively applied to shield steel substrates from hostile conditions including corrosive environments [5, 6]. As a physical barrier, epoxy coatings protect the metal surface from corrosive agents including ions, water, and oxygen [7]. The high cross-linking density of these coatings mostly explains their great mechanical integrity and resistance to permeation [8]. Coatings are not totally impervious, thus strong substances can still pass through them and cause deterioration over time [9]. Usually, the deterioration of epoxy coatings comes from the diffusion of corrosive agents into the polymer structure over extended exposure [10-12]. Hydroxyl ions (OH^-) produced at cathodic sites under the coating cause localized alkalinity increases (greater pH levels) under the coating interface [13]. This kind of pH change can greatly lower the adhesion strength between the coating and the substrate, so aggravating the corrosion process of the underlying metal [14].

The adhesion of epoxy coatings to the steel substrate greatly affects their corrosion-preventive qualities [15]. The interest in the development and enhancement of epoxy coatings has been increased owing to the increasing demand for protective coatings with improved performance and advancements in materials science. The most recent research advancements in epoxy coatings place a particular emphasis on their anticorrosive, thermal, and mechanical properties, as well as innovative modifications and additives designed to improve their overall efficacy [16, 17]. The application of the epoxy on the substrate surface can be executed deploying two techniques, specifically through spray and hand-roll techniques. Although numerous research methods employ these techniques for epoxy application on the substrate surface, research mostly prioritizes the impact of pre-treatment modifications on the substrate or that of modifications on the epoxy, such as the addition of organic and inorganic fillers, despite the critical nature of these application techniques.

The research on increasing the bond strength between the epoxy paint and substrate by modifying the substrate surface with the blasting method has been carried out. Authors in [18] investigated the effect of grinding and grit-blasting treatments on the bond-coat surface prior to top-coat deposition and the results show significantly reduced oxide growth. Furthermore, the benefits of blasting are underscored in [19], where it was emphasized that the quality of blasting directly influences the adhesion and service life of the coatings applied thereafter. This correlation illustrates the essential role that the surface preparation plays in the overall effectiveness of the epoxy coatings. Moreover, the presence of contaminants, such as residues left from the blasting process, can adversely affect the performance of the applied coating. In Contrast, authors in [20] noted that residual grit on the surface can degrade the service performance of coatings. Thus, a thorough cleaning process following blasting is often proposed to eliminate these residues before applying epoxy coatings [21]. Even though different pre-treatment methods were utilized, spray or handroll methods were employed during application. However, the effect of using these application methods on the quality of the coating results was not discussed.

Improving the quality of epoxy has also been explored in several existing studies, the majority of which propose the addition of fillers. The modification of epoxy coatings through this addition plays a crucial role in enhancing their physical and mechanical properties. Authors in [22] studied a handroll mixture of epoxy with halloysite nanotubes on the steel surface. The results exhibited that the addition of halloysite nanotubes loaded with sodium lignosulfonate has been shown to improve the corrosion resistance and to create a more complex microstructure that reduces the permeability to corrosive agents. Authors in [23] added molybdenum disulfide particles to the epoxy and then sprayed onto the surface of low carbon steel. It has been shown that incorporating alumina micro- and nanoparticles into epoxy coatings significantly enhances the mechanical and barrier properties of steel substrates [24]. The same research results were also found in [25], where ZnO was added. Authors in [26] used green inhibitors to overcome corrosion.

Research has mostly addressed changing the paint formulations, filler materials, curing methods, and substrate pre-treatment procedures. Notwithstanding these efforts, little has been known about how painting techniques affecting the coating performance. Although common coating techniques in industrial use are the spraying and handroll methods, specific scientific studies on their effects on the coating quality are still rare. Hence, this study's novelty lies in revealing the effect of the epoxy coating process on the coating performance deploying the spray and handroll methods. The basic physical phenomena that occur during the epoxy coating curing using the spray and handroll techniques are demonstrated. The former will be a foundation to understand the void formation on the epoxy.

The performed evaluation focused on revealing the effect of the spray and hand rolled coating methods and that of their combination on the epoxy coating regarding the pullout strength and corrosion characteristics. A pullout test was carried out to determine the bonding between the substrate and the paint. Meanwhile, potentiodynamic polarization testing was also conducted to determine the corrosion property response of the ASTM A36 steel, which was coated with epoxy when it was immersed in an environment containing chloride ions. This environment was chosen because chloride is the most aggressive and abundant ion in nature, while it contributes to steel degradation due to corrosion [27, 28]. The acronyms represent coating methods: S+S for spray primer and topcoat, H+H for handroll primer and topcoat, H+S for handroll primer with spray topcoat, and S+H for spray primer with handroll topcoat

II. MATERIALS AND METHODS

A. Materials

The water blasting was carried out using high-pressure mineral water, following garnet blasting with an 80-mesh particle size. Commercial Epoxy coat Interbond 201 by Akzo Nobel N.V Netherland was used in this study. The specimens were prepared using ASTM A36 steel, which was supplied by Krakatau Posco and had a composition of 0.26% C, 0.29% Si, 1.05% Mn, 0.04% P, and 0.07% S, with iron for balance (wt.%).

B. Surface Preparation and Coating Application

A test specimen of 200 mm × 200 mm × 5 mm size was made using low carbon ASTM A36 steel, followed by 500°C low temperature annealing for 1 h to remove the residual stress. The specimen was then sent to garnet blasting followed by water blasting with pressurized water jet 80 bar A 30-mesh garnet was used for sample preparation. The garnet blasting pressure was applied at 10 bar, maintaining a distance of 30 cm between the nozzle and the specimen. Each nozzle was positioned at a 90° angle to the surface of the specimen, and blasting was performed for 5 min. After water and garnet blasting, the specimen was dried using a dryer machine to ensure that no water remained on the surface, thus preventing flash corrosion. This is important to ensure that the surface of the specimen is clean from impurities before the coating process.

A specified quantity of epoxy resin, curing agent, and a suitable volume of ethanol (anhydrous) were all placed into the mixing container for thorough stirring (the percentage by weight of epoxy resin to the curing agent was 2:1) followed by the ultrasonic vibration process for 1 min to achieve a homogeneous mixture. Prior to the coating process, the environmental conditions were checked and conditioned. The recorded conditions were: Dry Bulb Temperature (Td) 31°C, Wet Bulb Temperature (Tw) 24°C, Relative Humidity (RH) 57%, Steel Temperature (ST) 24°C, and Dew Point 21°C. The prepared epoxy paint was then applied to the steel surface with three different methods: airless spray, handroll, and a combination of both. The thickness of the wet layer was maintained at 250±10 µm. The paint was then cured in an oven at 60 °C for 20 min for the first dry, and at room temperature for 6 h in the next curing step.

C. Surface Characterization

The surface morphology of the steel specimens coated with epoxy was examined using a Hitachi FlexSEM 1000 Scanning Electron Microscopy (SEM). SEM was conducted on the specimen's cross-section to analyze the characteristics of the sub-surface paint adhered to the substrate. The former was also carried out on the paint's surface to ascertain its detailed characteristics. SEM was conducted before and after exposure to the corrosive environment.

D. Pull Out Coating-Substrate Adhesion Characterization

The epoxy coating's adhesion to the substrates was evaluated using the Positest AT-M pull-off adhesion tester (DEFELSKO®) in accordance with ASTM D 4541 standards, as shown in Figure 1. The samples were measured prior to a 15-day immersion in seawater. The aluminum dollies were securely bonded to the epoxy-coated surface with Alteco adhesive. The samples were kept at room temperature for 24 h to ensure the complete curing of the glue. A slot was created around the dollies, which were then pulled at a speed of 10 mm/min, perpendicular to the coating surface, until the epoxy coating was separated from the steel substrate. Each test was conducted with three replicates to guarantee the consistency of the measurements. The Pullout strength value was calculated using:

$$\sigma = \frac{P}{A} \quad (1)$$

where σ is the pullout strength (MPa), P is the force applied to the dolly until break out (N), and A is surface area of the bottom of the dolly (mm^2). As the bottom of the dolly is circular, the area (A) can be determined using:

$$A = \frac{1}{4}\pi D^2 \quad (2)$$

where D is the diameter of the bottom of the dolly (mm) and π is 3.14159.

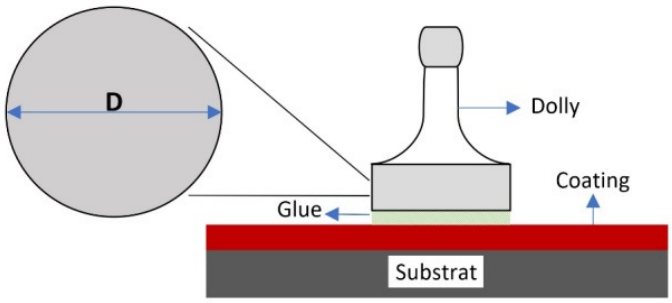

Fig. 1. Pullout test scheme.

E. Potentiodynamic Polarization Test Diagram

The epoxy coatings, applied to the surface-treated samples, were exposed and tested for their corrosion characteristics in seawater sourced from the Surabaya seashore in Indonesia. The potentiodynamic polarization technique (based on ASTM G59) was employed to examine the corrosion characteristics of the epoxy coating on the steel. The test scheme of potentiodynamic polarization technique is as displayed in Figure 2.

The experiment was conducted using a Palm sense Potentiostat-Galvanostat (Palm sense 4®, Netherland) at a swept rate of 1mV/s at room temperature conditions. The measurements were taken using a standard three-electrode cell, featuring a coated steel specimen as the working electrode, platinum (Pt) as the counter electrode, and Ag/AgCl as the reference electrode. Measurements were conducted on three samples to determine the standard deviations. The corrosion rate was calculated using (3):

$$CR = 0.00327\frac{i_{corr}xEW}{\rho} \quad (3)$$

where 0.00327 is the constant for CR in mm/ year, CR is the corrosion rate in mm/years, i_{corr} is the current density in µA/cm^2 measured using potentiostat devices, ρ is the material specific density, taken as 7.81 gr/cm^3 for A36 steel. The

Equivalent Weight (EW) of ASTM A36 steel was calculated using (4) and found to be 27.11.

$$EW = \frac{1}{\sum_1^z \frac{M_f x e_v}{A_r}} \quad (4)$$

where M_f is the mass fraction of the element base on the chemical composition, e_v are the valence electrons of each element, and A_r is the atomic weigh of each element.

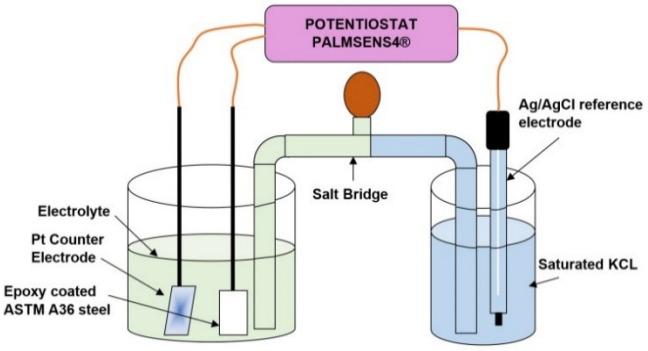

Fig. 2. Potentiodynamic polarization test scheme.

III. RESULT AND DISCUSSION

A. *Surface Optical Characterization*

The combination of garnet blasting followed by high-pressure water blasting produces a substrate that is well-prepared for coating. The results of this pre-treatment can be seen in Figure 3 (a). It is observed that the specimen before the treatment process appears severely rusty, but after the treatment, it is visibly clean, achieving a standard cleanliness level of G3 SP 5, as portrayed in Figure 3 (b). This shows that the combination of the garnet blasting and water blasting processes is very effective in cleaning the specimen surface from rust without leaving garnet residue on its surface.

The painting process was conducted on the specimen surface following the pre-treatment process. The surface of ASTM A36 steel was coated with epoxy coating using a various coating procedure, including rollers, sprays, and a combination of both. The results of the painting are depicted in Figure 4.

The thickness values of the paint measured using an Elcometer coating thickness gauge, are presented in Table I. The first and second layers of the paint are conditioned to have a thickness of 250-275 µm in wet-paint. Meanwhile, the thickness of the dry-paint can be observed to vary after the curing process and the paint has dried. Dry-paint coating using a spray has a greater thickness compared to the handroll process. In comparison, Spray-Spray (S+S) has a dry thickness of 129 µm, while Handroll-Handroll (H+S) has a thickness of 126 µm.

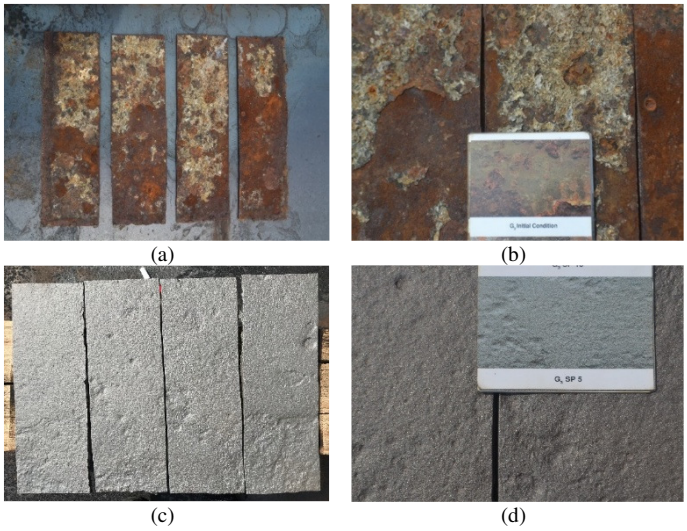

Fig. 3. Specimen of ASTM A36 steel: (a) and (b) before treatment, (c) and (d) after treatment by garnet blasting followed by hydroblasting.

Fig. 4. Epoxy coated ASTM A 36 steel.

TABLE I. COATING THICKNESS

Cote	Coating thickness 1st layer (µm)		Coating thickness 2nd layer (µm)	
	Wet	Dry	Wet	Dry
S + S	250 – 275	129	250 - 275	157
S + H	250 – 275	127	250 - 275	141
H + S	250 – 275	128	250 - 275	134
H + H	250 – 275	126	250 - 275	138

Consequently, S+S is 2.4% thicker than H+H. Compared to the hand roll method, the spray method in the painting procedure may result in lower paint density. This is because, during the spraying process, the paint adheres to the surface without any external force or surface pressure, the paint retains a micro-void space that is created during the painting process, increasing the paint's thickness.

Figure 5 shows the cross-section of the substrate A36 coated with Epoxy coating before being immersed in seawater. Even though there are no visible gaps or defects between the

paint layers, it can be seen that there is a boundary line between the first layer and the second layer for all painting methods. Figure 5 (a) presents the painting process using the S+S method. It can be seen that both layer one and layer two contain voids. The second layer is in contact with the free environment, but still the voids are unable to come out of the paint.

Figure 5 (b) displays a specimen using the first-layer spray and second-layer roll methods. In the layer coated with spray only, voids are present, whereas the layer coated using a roll is free of voids. This trend can also be seen in the Roll-Spray and Roll-Roll layers in Figures 5 (c) and (d), respectively, where the layers that use rolls are void free, while the layers that use spray contain voids.

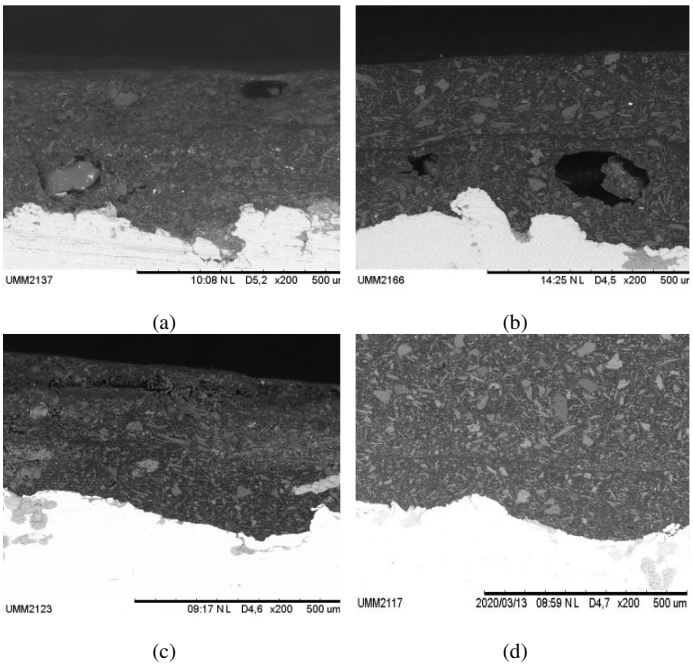

Fig. 5. Cross-section SEM of epoxy coated ASTM A36: (a) S+S; (b) S+H; (c) H+S; (d) H+H.

Figure 6 shows the surface condition of the paint on the substrate, before the corrosion process, for the variations of S+S, S+H, H+S, and H+H applications. It can be seen that the appearance of the surface of the substrate using the S+S and H+S methods shows small holes or voids on the surface, while the substrate painted using S+H and H+H appears more solid with no voids. These voids are likely formed due to trapped air during painting. In the painting process using spray there are air particles that are also painted and stuck to the surface of the substrate. The spray process can also cause rapid drying due to the presence of air, which results in forced convection during the curing process. An illustration of the drying process with solvent mass transfer is provided in Figure 7.

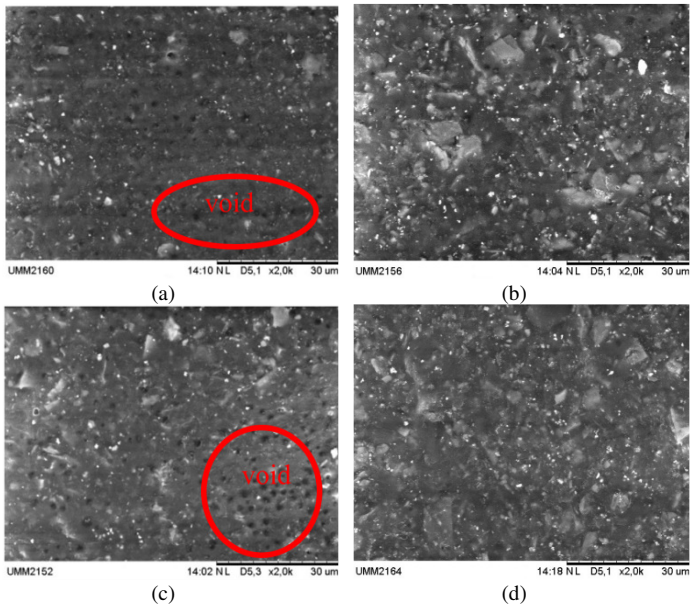

Fig. 6. Surface SEM of epoxy coated ASTM A36: (a) S+S; (b) S+H; (c) H+S; (d) H+H.

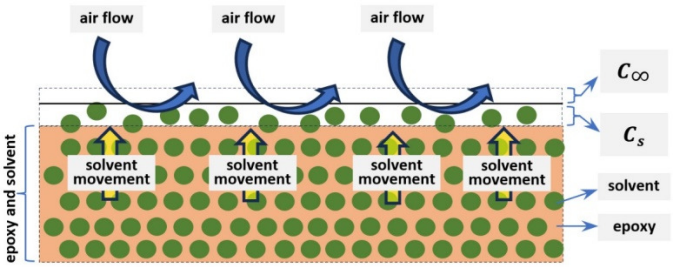

Fig. 7. Proposed model of solvent mass transfer during epoxy drying.

In figure 7, C_s is the solvent concentration right at the air interface and the paint surface, while C_∞ is the solvent concentration far above the paint surface. The drying process of the epoxy coating can be formulated using diffusion from Fick's law and is described diagrammatically in Figure 8.

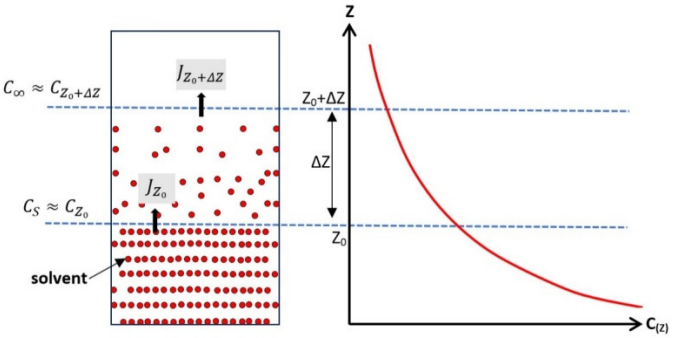

Fig. 8. Proposed mathematic model of epoxy coating drying process using Fick Law.

If the solvent evaporates from the paint in a volume of $\Delta V=A\ \Delta Z$, then the mass entering ΔV at Z_0 with a time interval of Δt can be formulated as:

$$m_{Z_0} = J_{Z_0} A \, \Delta t \quad (5)$$

where m_{Z_0} is the mass of the solvent that comes out of the paint and enters the thin layer right above the paint along ΔZ, A is the area of the sample, and J_{Z_0} is the solvent mass transfer flux at Z_0. The mass exiting ΔV at at position $Z_0+\Delta Z$ during the same time interval Δt is denoted as $m_{Z_0+\Delta Z}$ and is formulated as:

$$m_{Z_0+\Delta Z} = J_{Z_0+\Delta Z} A \, \Delta t \quad (6)$$

where $J_{Z_0+\Delta Z}$ is the solvent mass transfer flux at $Z_0+\Delta Z$. Meanwhile, the mass accumulated (Δm) in ΔV at time Δt can be formulated as:

$$\Delta m = m_{Z_0} - m_{Z_0+\Delta Z} \quad (7)$$

$$\Delta m = (J_{Z_0} A \, \Delta t) - (J_{Z_0+\Delta Z} A \, \Delta t) \quad (8)$$

$$\Delta m = (A \, \Delta t)(J_{Z_0} - J_{Z_0+\Delta Z}) \quad (9)$$

$$\Delta m = (J_{Z_0+\Delta Z} - J_{Z_0})(A \, \Delta t) \quad (10)$$

$$\Delta m = \Delta J \, A \, \Delta t \quad (11)$$

The change in the solvent concentration ΔC is given by:

$$\Delta C = \frac{\Delta m}{\Delta V} \quad (12)$$

$$\Delta C = \frac{\Delta J \, A \, \Delta t}{A \, \Delta Z} \quad (13)$$

$$\frac{\Delta C}{\Delta t} = \frac{\Delta J}{\Delta Z} \quad (14)$$

It is evident from (14) that an increase in the change of concentration over time $\Delta C/\Delta t$ corresponds to a higher gradient of mass flux over distance $\Delta J/\Delta Z$, indicating an enhanced rate of mass transfer. When air is blown across the paint surface, the air containing solvent vapor is rapidly replaced by fresh, dry air, maintaining a low ambient concentration of solvent vapor C_∞. This condition sustains a high concentration gradient between the paint surface and the surrounding air, which in turn increases the solvent evaporation rate. As a result, the paint dries more quickly. However, this rapid drying may trap water vapor bubbles within the paint film before they can escape, potentially affecting the coating quality.

The proposed model was validated qualitatively by examining the surface morphology using SEM. Although, direct experimental measurements of mass transfer flux were not conducted, the SEM analysis provided clear evidence supporting the theoretical predictions. The SEM images revealed distinct variations in the void formations on the epoxy coating surfaces, corresponding directly to differences in the employed drying processes. These void structures are indicative of the underlying mass transfer phenomena and illustrate differences in the solvent evaporation rates, aligning well with the predictions made by the proposed model. Thus, the observed correlation between the predicted drying behavior and the actual surface morphology confirms the reliability and accuracy of the proposed theoretical framework.

B. Pull Out Strength Analysis

Table II presents the pullout strength results of the epoxy coating on ASTM A36 steel, arranged based on various coating application techniques, combining S+H methods for the primer and topcoat layers. The macro image of the pullout results is presented in Figure 9. Variations in adhesion strength under the influence of the coating application technique were found by the pull-out strength test. The specimen with handroll primer and spray topcoat showed the highest pullout strength 13.05 MPa, while the spray primer and handroll topcoat (S+H) had the lowest strength of 5.40 MPa.

TABLE II. PULL OUT TEST RESULT OF EPOXY COATED A36 STEEL

Code	Pullout strength (MPa)	Failure mode (%)
S + S	7.35	B = 55; C=45
S + H	5.40	B = 80; C=20
H + S	13.05	B =20; C=70 ; Y/Z=10
H + H	11.41	C=20; Y/Z=80

*S = Spray; H = Hand Roll; A = ASTM A36 base metal; B = Primer coating; C = Top Coating; Y/Z = Glue.

A rather moderate pullout strength of 7.35 MPa was observed in the S+S specimen together with a virtually balanced failure between topcoat (45%) and primer (55%). The spray-applied coatings typically exhibit lower adhesive strength due to the higher porosity and void content. This spray technique usually generates thinner, more porous layers, which reduces the adhesive strength between the primer and substrate. The weakest specimen (S+H) primarily failed within the primer layer, with approximately 80% of the failure occurring there. This suggests inadequate adhesion between the spray primer and substrate. These findings align with previous studies, which reported reduced interfacial bonding when spray primers were used. On the other hand, the topcoat applied with the handroll technique had a denser coverage and reduced void presence, and hence directed the failure mostly toward the primer interface.

Using the handroll application technique, which is known for generating thicker and denser coatings with enhanced mechanical interlocking, specimen H+S, demonstrated the highest pullout strength and had a strong primer-substrate adhesion. Specimen H+S mostly failed in the spray topcoat layer (70%), suggesting higher porosity in the spray-applied coating, which is consistent with research indicating that the spray coatings exhibit more void spaces. Glue failure (10%) indicates a thin adhesive penetration into the surface voids, facilitating the mechanical bonding. The H+H specimen displayed great strength (11.41 MPa) with failure mostly in glue adhesion (80%), underlining that both the primer and topcoat layers applied by the handroll techniques achieved excellent adhesion quality. Therefore, the adhesive used in the pullout testing becomes the weakest link. The hand-applied coatings produced smoother surfaces with fewer voids, significantly improving the inter-layer adhesion.

C. Corrosion Analysis

Figure 10 illustrates the potentiodynamic polarization curves for the epoxy-coated ASTM A36 steel specimens exposed to sea water.

In addition to the corrosion rate and current density analysis, the nobility of the material can also be evaluated from the potentiodynamic polarization results, particularly by

observing the corrosion potential (E_{corr}). Materials with a more positive (or less negative) E_{corr} are considered more noble, indicating a higher resistance to oxidation or a lower tendency to corrode in the given environment. This trend in nobility correlates with the observed corrosion behavior and further supports the effectiveness of the coating in enhancing the corrosion resistance. The results of corrosion test indicate that the E_{corr} values of the tested specimens varied significantly, reflecting differences in electrochemical stability.

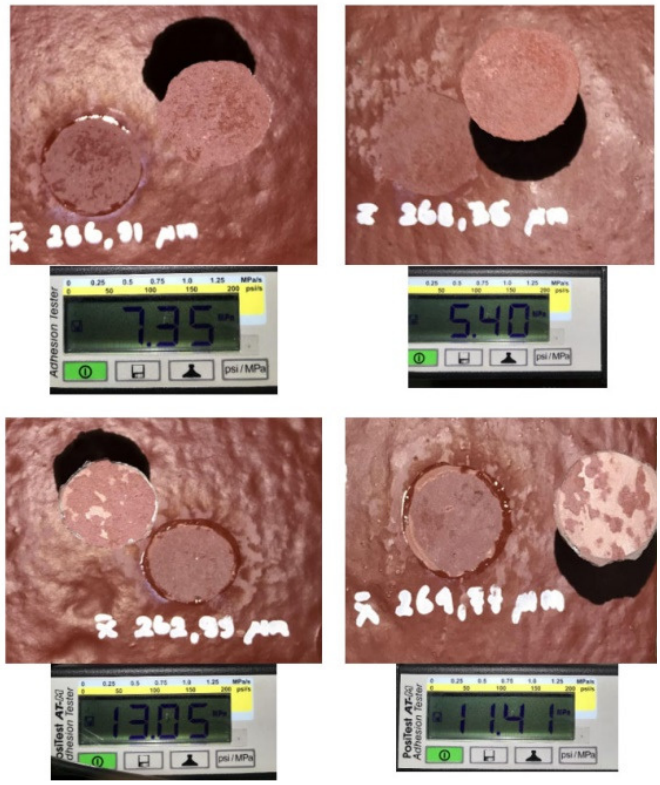

Fig. 9. Macro observation of pullout test results.

As seen in Figure 10, specimen S+S exhibited the most negative corrosion potential (-1085 mV), indicating the highest susceptibility to corrosion. The specimens S+H (-931 mV) and H+S (-865 mV) displayed an improved corrosion potential. Notably, Specimen H+H (-647 mV) presented the most positive corrosion potential, suggesting superior resistance to corrosion among the evaluated samples. The corrosion current density also changes due to differences in the coating methods. The greatest current density was found in specimens coated with the S+Smethod, while the smallest current density occurs in the H+H method. The decrease in corrosion current density can be attributed to the fewer voids in the H+H specimen; with less area exposed to the electrolyte, the resulting corrosion current density is also lower. The smaller the corrosion current density is, the lower is the corrosion rate, as the latter is calculated based on the corrosion current density variable, as mentioned in the method.

The observed corrosion mechanism in ASTM A36 steel coated with epoxy when exposed to a seawater (chloride rich) environment involves several electrochemical processes. Initially, chloride ions (Cl^-) penetrate the epoxy coating through inherent micropores, voids, and defects, reaching the steel substrate. The presence of voids within the coating structure significantly affects the corrosion process, as they serve as pathways for aggressive ion penetration. The dissolution of Fe takes place due to thermodynamic and electrochemical driving forces.

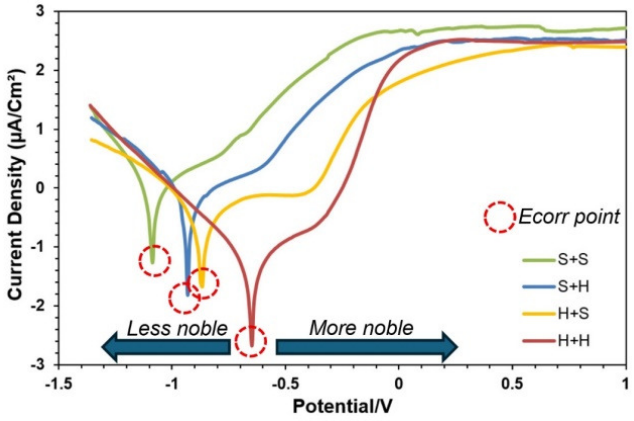

Fig. 10. Potentiodynamic polarization test results of epoxy coated A36 steel.

This ionic penetration facilitates the direct electrochemical interactions between the steel surface and electrolyte, leading to anodic dissolution of the Fe as the main composition of A36 steel. Figure 11 illustrates the corrosion mechanism of the specimen A36 coated with epoxy coating.

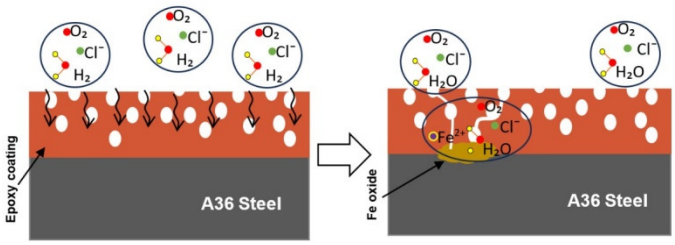

Fig. 11. Corrosion of the epoxy coating model.

This process is primarily governed by the electrochemical potential of iron, the presence of an electrolyte, and the formation of a galvanic cell on the metal surface, the reaction can be represented as:

$$Fe \rightarrow Fe^{2+} + 2e^- \quad E = -0.44V \tag{15}$$

A negative electrode potential means that Fe tends to be easier to lose electrons and dissolve into the electrolyte as Fe^{2+}. The electrons released by Fe are utilized by the cathode for the reduction reaction. In general, the reduction reaction at the cathode involves O_2 and H_2O, the reaction can be presented as:

$$O_2 + H_2O + 4e^- \rightarrow 4OH^- \quad E = +0.4V \tag{16}$$

This reaction causes the oxidation reaction in Fe to occur spontaneously because the reaction potential in Fe is more negative than that of the oxygen reduction reaction.

Fe^{2+} ions then react with hydroxide ions (OH^-) to form iron hydroxide; the reaction can be described as:

$$Fe^{2+} + 2OH^- \rightarrow Fe(OH)_2 \quad (17)$$

The $Fe(OH)_2$ is known as the corrosion product. The above reaction occurs if the epoxy can be penetrated by the electrolyte and results in a redox reaction.

The reaction is faster with the presence of chloride ions as a catalyst. Chloride ions Cl^- do not participate directly in the electrochemical reaction, but have an important role in keeping iron Fe^{2+} ions in the solution. Usually, Fe^{2+} forms an oxide layer, such as $Fe(OH)_2$. However, the chloride ions inhibit the formation of this oxide layer by forming a complex with the iron ions:

$$Fe^{2+} + 4Cl^- \rightarrow (FeCl_4)^{2-} \quad (18)$$

$(FeCl_4)^{2-}$ dissolves in water and inhibits Fe^{2+} from forming an oxide layer on the surface of the substrate. As a result, corrosion continues in the absence of this protective layer. It is well known that the oxide layer prevents the electrolyte from reaching the metal surface, thereby reducing the corrosion rate.

IV. CONCLUSSION

The present study assessed the effects of the epoxy coating application techniques, namely spray, handroll, and their combinations on ASTM A36 steel substrates. Pullout tests found that the handroll primer combined with spray topcoat (H+S) produced the highest adhesion strength (13.05 MPa), ascribed in part to its dense, void-free primer that improved the mechanical interlocking and chemical bonding with the substrate. Because of considerable void development in the spray-applied primer layer, the spray primer combined with the handroll topcoat (S+H) showed the lowest adhesion strength (5.40 MPa).

With the most positive corrosion potential (-647 mV), which indicates fewer voids and lessened chloride ion penetration, the potentiodynamic polarization tests revealed that the coatings applied only by handroll (H+H) had a superior corrosion resistance. In contrast, the coatings applied entirely by spraying (S+S) showed the highest corrosion sensitivity. These results highlight the need to choose suitable painting techniques to minimize the flaws and maximize the coating adhesion and anti-corrosion performance, especially in handroll applications.

ACKNOWLEDGMENT

The authors would like to express their deepest gratitude to the Ministry of Research and Higher Education of the Republic of Indonesia for their financial support and valuable guidance during this research process. The authors gratefully acknowledge Universitas Brawijaya for the facilities provided.

REFERENCES

[1] G. Cui *et al.*, "A comprehensive review on smart anti-corrosive coatings," *Progress in Organic Coatings*, vol. 148, Nov. 2020, Art. no. 105821, https://doi.org/10.1016/j.porgcoat.2020.105821.

[2] A. Pistone, C. Scolaro, and A. Visco, "Mechanical Properties of Protective Coatings against Marine Fouling: A Review," *Polymers*, vol. 13, no. 2, Jan. 2021, Art. no. 173, https://doi.org/10.3390/polym13020173.

[3] T. Ramakrishnan *et al.*, "Study of Various Epoxy-Based Surface Coating Techniques for Anticorrosion Properties," *Advances in Materials Science and Engineering*, vol. 2022, pp. 1–8, Jan. 2022, https://doi.org/10.1155/2022/5285919.

[4] J. R. Xavier, "Superior Surface Protection, Mechanical and Hydrophobic Properties of Silanized Tungsten Carbide Nanoparticles Encapsulated Epoxy Nanocomposite Coated Steel Structures in Marine Environment," Silicon, vol. 14, no. 17, pp. 11147–11161, Nov. 2022, https://doi.org/10.1007/s12633-022-01842-0.

[5] E. Amendola, B. Palmieri, S. Dello Iacono, and A. Martone, "Thermally Mendable Self-Healing Epoxy Coating for Corrosion Protection in Marine Environments," *Materials*, vol. 16, no. 5, Feb. 2023, Art. no. 1775, https://doi.org/10.3390/ma16051775.

[6] I. Chopra, S. K. Ola, Priyanka, V. Dhayal, and D. S. Shekhawat, "Recent advances in epoxy coatings for corrosion protection of steel: Experimental and modelling approach-A review," *Materials Today: Proceedings*, vol. 62, pp. 1658–1663, 2022, https://doi.org/10.1016/j.matpr.2022.04.659.

[7] B. Ou, Y. Wang, and Y. Lu, "A review on fundamentals and strategy of epoxy-resin-based anticorrosive coating materials," *Polymer-Plastics Technology and Materials*, vol. 60, no. 6, pp. 601–625, Apr. 2021, https://doi.org/10.1080/25740881.2020.1819317.

[8] J. Y. Zhang, B. Xu, N. Haq Tariq, M. Sun, D. Li, and Y. Y. Li, "Microstructure evolutions and interfacial bonding behavior of Ni-based superalloys during solid state plastic deformation bonding," *Journal of Materials Science & Technology*, vol. 46, pp. 1–11, June 2020, https://doi.org/10.1016/j.jmst.2019.11.015.

[9] K. B. Tator and R. Lanterman, "Coating Deterioration - a Mechanistic Overview," in *CORROSION 2016*, Vancouver, BC, Mar. 2016, pp. 1–12, https://doi.org/10.5006/C2016-07065.

[10] S. Anwar and X. Li, "A review of high-quality epoxy resins for corrosion-resistant applications," *Journal of Coatings Technology and Research*, vol. 21, no. 2, pp. 461–480, Mar. 2024, https://doi.org/10.1007/s11998-023-00865-5.

[11] M. Shen and M. L. Robertson, "Degradation Behavior of Biobased Epoxy Resins in Mild Acidic Media," *ACS Sustainable Chemistry & Engineering*, vol. 9, no. 1, pp. 438–447, Jan. 2021, https://doi.org/10.1021/acssuschemeng.0c07621.

[12] H. Zargarnezhad, E. Asselin, D. Wong, and C. N. C. Lam, "A Critical Review of the Time-Dependent Performance of Polymeric Pipeline Coatings: Focus on Hydration of Epoxy-Based Coatings," *Polymers*, vol. 13, no. 9, May 2021, Art. no. 1517, https://doi.org/10.3390/polym13091517.

[13] C. Xing, W. Wang, S. Qu, Y. Tang, X. Zhao, and Y. Zuo, "Degradation of zinc-rich epoxy coating in 3.5% NaCl solution and evolution of its EIS parameters," *Journal of Coatings Technology and Research*, vol. 18, no. 3, pp. 843–860, May 2021, https://doi.org/10.1007/s11998-020-00448-8.

[14] L. Ma *et al.*, "Self-reporting coatings for autonomous detection of coating damage and metal corrosion: A review," *Chemical Engineering Journal*, vol. 421, no. 02, Oct. 2021, Art. no. 127854, https://doi.org/10.1016/j.cej.2020.127854.

[15] S. G. Croll, "Surface roughness profile and its effect on coating adhesion and corrosion protection: A review," *Progress in Organic Coatings*, vol. 148, Nov. 2020, Art. no. 105847, https://doi.org/10.1016/j.porgcoat.2020.105847.

[16] S. M. Chhipa, S. Sharma, and A. Kumar Bagha, "Recent development in polymer coating to prevent corrosion in metals: A review," *Materials Today: Proceedings*, Oct. 2024, Art. no. S2214785324004851, https://doi.org/10.1016/j.matpr.2024.09.001.

[17] Y. Qian, Y. Li, S. Jungwirth, N. Seely, Y. Fang, and X. Shi, "Review: The Application of Anti-Corrosion Coating for Preserving the Value of Equipment Asset in Chloride-Laden Environments: A Review," *International Journal of Electrochemical Science*, vol. 10, no. 12, pp. 10756–10780, Dec. 2015, https://doi.org/10.1016/S1452-3981(23)11298-3.

[18] K. Ito, T. Shima, M. Fujioka, and M. Arai, "Improvement of Oxidation Resistance and Adhesion Strength of Thermal Barrier Coating by Grinding and Grit-Blasting Treatments," *Journal of Thermal Spray Technology*, vol. 29, no. 7, pp. 1728–1740, Oct. 2020, https://doi.org/10.1007/s11666-020-01057-y.

[19] M. Li, J. Huang, S. Li, M. Peng, Z. Yan, and Q. Song, "Research on quality inspection and process optimization of ship surface shot blasting and sand blasting treatment," *Journal of Physics: Conference Series*, vol. 2775, no. 1, June 2024, Art. no. 012044, https://doi.org/10.1088/1742-6596/2775/1/012044.

[20] D. Ye *et al.*, "Prediction and Analysis of the Grit Blasting Process on the Corrosion Resistance of Thermal Spray Coatings Using a Hybrid Artificial Neural Network," *Coatings*, vol. 11, no. 11, Oct. 2021, Art. no. 1274, https://doi.org/10.3390/coatings11111274.

[21] A. Marques *et al.*, "Review on Adhesives and Surface Treatments for Structural Applications: Recent Developments on Sustainability and Implementation for Metal and Composite Substrates," *Materials*, vol. 13, no. 24, Dec. 2020, Art. no. 5590, https://doi.org/10.3390/ma13245590.

[22] D. Yan *et al.*, "Smart self-healing coating based on the highly dispersed silica/carbon nanotube nanomaterial for corrosion protection of steel," *Progress in Organic Coatings*, vol. 164, Mar. 2022, Art. no. 106694, https://doi.org/10.1016/j.porgcoat.2021.106694.

[23] G. Zhou *et al.*, "Surface modified molybdenum disulfide nanosheets for corrosion resistance improvement on polyurethane coatings," *Corrosion Reviews*, vol. 42, no. 4, pp. 485–496, Aug. 2024, https://doi.org/10.1515/corrrev-2023-0119.

[24] D. Saber *et al.*, "Enhancement of Barrier and Mechanical Performance of Steel Coated with Epoxy Filled with Micron and Nano Alumina Fillers," *Materials Research*, vol. 25, 2022, Art. no. e20210413, https://doi.org/10.1590/1980-5373-mr-2021-0413.

[25] N. F. Ibrahim, W. R. Wan Abdullah, M. S. Rooshde, M. S. Mohd Ghazali, and W. N. W. Mohd Norsani, "Corrosion Inhibition Properties of Epoxy-Zinc Oxide Nanocomposite Coating on Stainless Steel 316L," *Solid State Phenomena*, vol. 307, pp. 285–290, July 2020, https://doi.org/10.4028/www.scientific.net/SSP.307.285.

[26] M. I. Haris, Agung, M. Anjas, G. J. B. Houston, N. Qadry, and Fakhruddin, "Development of a Green Corrosion Inhibitor from Lophatherum Gracile Extract for Steel Protection," *Engineering, Technology & Applied Science Research*, vol. 15, no. 1, pp. 19253–19260, Feb. 2025, https://doi.org/10.48084/etasr.8609.

[27] D. Aroussi, B. Aour, and A. S. Bouaziz, "A Comparative Study of 316L Stainless Steel and a Titanium Alloy in an Aggressive Biological Medium," *Engineering, Technology & Applied Science Research*, vol. 9, no. 6, pp. 5093–5098, Dec. 2019, https://doi.org/10.48084/etasr.3208.

[28] F. B. Mainier, A. M. Coelho, and E. F. Barros, "Corrosivity Evaluation of Copper-Nickel Alloy (90/10) in Pumps Used in Offshore Platforms for Seawater Pumping," *Engineering, Technology & Applied Science Research*, vol. 9, no. 5, pp. 4636–4639, Oct. 2019, https://doi.org/10.48084/etasr.3016.